Published in IET Control Theory and Applications
Received on 20th July 2010
Revised on 25th April 2011
doi: 10.1049/iet-cta.2010.0415

ISSN 1751-8644

Adaptive robust control for DC motors with input saturation

Z. Li[1,2] *J. Chen*[2] *G. Zhang*[2] *M.G. Gan*[2]

[1]*Beijing Institute of Control Engineering, 100080, People's Republic of China*
[2]*Beijing Key Laboratory of Automatic Control System, Beijing Institute of Technology, Beijing 100081, People's Republic of China*
E-mail: lizplst@gmail.com

Abstract: The adaptive robust control (ARC) for DC motors subjected to parametric uncertainties, disturbances and input saturation is considered in this study. To achieve high performance while keeping the control authority within saturation limit, a saturated ARC scheme is proposed. In this scheme, a variable-gain saturation function is introduced for the virtual control law, so that the amplitude of the virtual control and its derivative decrease when the control input approaches to the prescribed bound. Consequently, the virtual control and its derivative will not be excessively large, which is crucial for stabilising the system with a bounded input. We prove that the proposed controller cannot only assure global stability, but also provide desirable control performance, that is, the tracking error can be steered to the neighbourhood of the origin in finite time. Moreover, asymptotic tracking can be achieved in the presence of parametric uncertainties only. Finally, simulation results illustrate the effectiveness of the proposed controller.

1 Introduction

Input saturation is one of the most common non-linearities in physical systems, which can be found in almost all actuators. If the system operates with a control input beyond the saturation limit, deteriorated control performance appears, and even instability of the close loop occurs [1, 2]. Therefore the control problem of plants with saturation attracts much attention and research articles in the last decades contain a significant amount of new knowledge [3]. In [4], the controller design of a linear stable plant with input saturation is directly solved by a linear matrix inequality optimisation approach. In [5], composite quadratic Lyapunov function is utilised to construct the control law for linear plants subjected to input constraint. In [6], a novel saturated control structure was proposed to ensure the globally asymptotic stability using a set of linear coordinate transformations and multiple saturation-type functions.

However, all the above results are based on the assumption that the plants are linear and exactly known, which is not satisfied in many applications. Taking servo systems for instance, the friction non-linearity, disturbance and parametric uncertainties influence the control performance [7]. It is necessary to consider these uncertainties when coping with the actuator saturation problem.

In order to improve the control performance of the uncertain non-linear systems, an adaptive robust control (ARC) method was proposed by Yao [8, 9]. It is performance-oriented and has strong performance in robustness [10–12]. However, in the traditional ARC the input saturation is rarely considered. Although the projection-type adaptation of ARC can alleviate integral windup problem caused by parameter adaptations [13], the previous ARC strategy [8, 9] does not guarantee global stability when the actuator saturation exists.

To solve this problem, Gong and Yao [14] combined the nested saturated control design [6] and the ARC approach to achieve both global stability and high performance for the plants subjected to the matched parametric uncertainty and disturbance. Nevertheless, this method is based on a transformed state-space model, in which the model uncertainties have direct influence on every state. Hence, the resulting controller is usually conservatively designed to handle the enlarged model uncertainties. In [15, 16], Hong and Yao also investigated the ARC design for linear motors with input saturation. They introduced saturation functions to construct the (virtual) control law in each recursive backstepping procedure, so that the output of the adaptive robust controller is bounded. However, in this method since the gain of virtual control is fixed, the derivative of virtual control may become excessively large, then a large control input is required to dominate the derivative of virtual control. In order to assure the stability of the close loop while keeping the control input within the limit, the gain of virtual control is constrained, and then the tracking error for virtual control, that is, $|z_2|$ cannot be monotonically decreasing. That means the final control law may be conservative.

In this paper, we propose a saturated adaptive robust control (SARC) scheme to achieve high performance while considering the input saturation of the plant. To make the saturated controller less conservative, a variable-gain

saturation function in the virtual control law is introduced. Therefore the magnitude of virtual control and its derivative decrease when the control input gets close to the prescribed bound and the control saturation is avoided effectively. Moreover, comparing with the controller proposed in [15], the design procedure of our controller is more flexible, which leads to less conservative performance.

This paper is organised as follows. The problem description is presented in Section 2. The design procedure of the proposed SARC is provided in Section 3. The stability proof and performance analysis are given in Section 4. Simulations are described and analysed in Section 5 and conclusions are outlined in Section 6.

2 Dynamic models and problem formulations

2.1 Dynamic model of servo mechanisms

The control of DC motors subjected to input saturation are investigated. The mechanical dynamics of a servo mechanism can be described by

$$J\ddot{q} + T_{\mathrm{f}} + T_{\mathrm{l}} + T_{\mathrm{dis}} = T_{\mathrm{m}} \tag{1}$$

where J is the inertial sum of load and armature; q is the motor output angle; T_{m} is the electromagnetic torque; T_{f} is the friction torque; T_{l} is the unknown payload; T_{dis} is the torque disturbance. In this paper, a simple friction model described by the Coulomb plus viscous model [17] is considered.

$$T_{\mathrm{f}}(\dot{q}) = T_{\mathrm{c}}\mathrm{sgn}(\dot{q}) + B\dot{q} \tag{2}$$

In this equation, T_{c} is the level of Coulomb friction torque, B is the viscous friction coefficient and the signum function $\mathrm{sgn}(\bullet)$ is defined by

$$\mathrm{sgn}(\bullet) = \begin{cases} 1, & \bullet > 0 \\ 0, & \bullet = 0 \\ -1, & \bullet < 0 \end{cases}$$

From (1) and (2), one has

$$J\ddot{q} + B\dot{q} = T_{\mathrm{m}} - T_{\mathrm{c}}\ \mathrm{sgn}(\dot{q}) - T_{\mathrm{l}} - T_{\mathrm{dis}}s \tag{3}$$

The electromagnetic torque T_{m} in (1) is given by

$$T_{\mathrm{m}} = K_T i \tag{4}$$

where K_T is the force constant. The current dynamics of a servo mechanism can be modelled as

$$L\mathrm{d}i/\mathrm{d}t + iR + K_{\mathrm{E}}\dot{q} = \mathrm{sat}(u, M_u) \tag{5}$$

In (5), R and L are the resistance and induction of the armature, respectively; i is the motor current amplitude; K_{E} is the electromotive force coefficient; u is the input voltage; M_u is the amplitude boundary of the input voltage; sat is the saturation function, which is defined as

$$\mathrm{sat}(u, M_u) = \begin{cases} M_u & u > M_u \\ u & -M_u \le u \le M_u \\ -M_u & u < -M_u \end{cases} \tag{6}$$

In general, the electrical constant L/R is small (compared to the mechanical time constant J/B), therefore from (3)–(5), we know that the electrical transients decay quite rapidly and $L\mathrm{d}i/\mathrm{d}t$ is very close to zero [18]. Thus, the dynamics of a servo mechanism can be simplified as [19]

$$\ddot{q} = \frac{K_1}{J}\mathrm{sat}(u, M_u) - \frac{K_2}{J}\dot{q} - \frac{T_{\mathrm{c}}}{J}\mathrm{sgn}(\dot{q}) - \frac{1}{J}(T_{\mathrm{l}} + T_{\mathrm{dis}}) \tag{7}$$

where

$$K_1 = K_{\mathrm{T}}/R, \quad K_2 = (K_{\mathrm{T}}K_{\mathrm{E}} + BR)/R \tag{8}$$

As seen, the DC motor model (7) is second order with nonlinearity and disturbance.

Herein, we use a continuous function S_{f} to approximate the discontinuous function $\mathrm{sgn}(x_2)$ [20]. The angle q is regarded as the system output y and the system state vector is defined by $[x_1, x_2]^{\mathrm{T}} = [q, \dot{q}]^{\mathrm{T}}$. Define T_n as the mean value of $T_{\mathrm{l}} + T_{\mathrm{dis}}$ and Δ as the lumped disturbance, that is, $\Delta = (T_{\mathrm{l}} + T_{\mathrm{dis}} - T_n + T_{\mathrm{c}}(\mathrm{sgn}(x_2) \times S_{\mathrm{f}}))/J$. Then, from (7), the following state-space form of the DC motor model can be obtained.

$$\begin{cases} \dot{x}_1 = x_2 \\ \dot{x}_2 = C \cdot \bar{u} - \theta_1 x_2 - \theta_2 S_{\mathrm{f}} + \theta_3 + \Delta \\ y = x_1 \\ \bar{u} = \mathrm{sat}\,(u, M_u) \end{cases} \tag{9}$$

where C and $\theta_j (j = 1, 2, 3)$ are defined as follows

$$\begin{aligned} &\Delta = \frac{d}{J}(\mathrm{rad/s^2}), \quad C = \frac{K_1}{J}((\mathrm{rad/s^2})/\mathrm{v}) \\ &\theta_1 = \frac{K_2}{J}(1/\mathrm{s}), \quad \theta_2 = \frac{T_{\mathrm{c}}}{J}((\mathrm{rad/s^2})/(\mathrm{N \cdot m})), \\ &\theta_3 = \frac{T_n}{J}(\mathrm{rad/s^2}) \end{aligned} \tag{10}$$

2.2 Assumptions and problem formulations

For simplicity, the following notations will be used: $\bullet_j$ for the jth component of the vector $\bullet$, $\hat{\bullet}$ for the estimate of $\bullet$, $\bullet_{\min}$ for the minimum value of $\bullet$, and $\bullet_{\max}$ for the maximum value of $\bullet$. The operation $\le$ for two vectors is performed in terms of the corresponding elements of the vectors.

Assumption 1: The parameter C in (9) is known and the extent of the unknown parameter θ_j, $j = 1, 2, 3$ is known, that is, $0 < \theta_{j\min} \le \theta_j \le \theta_{j\max}$, where $\theta_{j\min}$ and $\theta_{j\max}$ are known.

Remark 1: This assumption is reasonable and of practical significance, because the two parameters (K_1 and J) are more unlikely to change during a single operation in comparison with other parameters and can normally be estimated accurately online [15]. Thus, we assume that the parameter C in (9) is constant and known according to (10). In addition, to determine the bounds $\theta_{j\min}$ and $\theta_{j\max}$, the rough value of θ_j can be obtained first from the product specifications or the off-line system identification. Then the lower and upper bounds can be set as less and more than 10 or 50% of this value, respectively.

Assumption 2: The disturbance Δ is bounded, that is, $|\Delta| \le \delta$, where δ is some positive constant.

IET Control Theory Appl., 2011, Vol. 5, Iss. 16, pp. 1895–1905
doi: 10.1049/iet-cta.2010.0415

With the dynamic models and assumptions above, the control problem of this paper can be stated as follows: Given the desired motion trajectory $x_{1d}(t)$ which is bounded with bounded derivatives up to the second order, the objective is to synthesise a control input u such that the output $y = x_1$ tracks $x_{1d}(t)$ as close as possible, while the input u remains in the prescribed bound $[-M_u, M_u]$.

3 ARC design for servo mechanisms with input saturation

To solve the aforementioned control problem, a SARC method is proposed. The concrete design procedure is given as follows:

Step 1: Define a variable z_1 as

$$z_1 = x_1 - x_{1d} \tag{11}$$

Here, z_1 represents the output tracking error. From (9), we know $\dot{z}_1 = x_2 - \dot{x}_{1d}$. In this step, we need to synthesise a virtual control law α_1 satisfying these conditions: (i) The tracking error z_1 converges to zero globally when $x_2 = \alpha_1$. (ii) α_1 should be bounded, which is necessary for the boundedness of the control input u. In view of the above two conditions, we design the virtual control law α_1 as

$$\alpha_1 = \dot{x}_{1d} - \sigma_1(z_1, z_2) \tag{12}$$

where z_2 is given by

$$z_2 = x_2 - \alpha_1 \tag{13}$$

and $\sigma_1(z_1, z_2)$ is

$$\sigma_1(z_1, z_2) = \sigma_{11}(z_1) \cdot \sigma_{12}(z_2) \tag{14}$$

where σ_{11} and σ_{12} are smooth functions with available first-order derivatives defined as follows:

1. The definition of σ_{11} is

$$\sigma_{11}(z_1) = \begin{cases} -M_1 & z_1 < -L_{12} \\ 0.5a(z_1 + L_{12})^2 - M_1 & -L_{12} \le z_1 < -L_{11} \\ k_1 z_1 & -L_{11} \le z_1 < L_{11} \\ -0.5a(L_{12} - z_1)^2 + M_1 & L_{11} \le z_1 < L_{12} \\ M_1 & L_{12} \le z_1 \end{cases} \tag{15}$$

where $L_{12} = (M_1/k_1) + (k_1/2a)$ and $L_{11} = L_{12} - (k_1/a)$. In (15), M_1, a, k_1 are positive design parameters satisfying

$$2M_1 a > k_1^2 \tag{16}$$

which yields $L_{11} > 0$, and then $\sigma_{11}(z_1)$ is well defined. From (15), it is easy to check that $\sigma_{11}(z_1)$ is a smooth saturated function. Furthermore, it has a continuous first-order derivative below

$$\frac{\mathrm{d}\sigma_{11}(z_1)}{\mathrm{d}z_1} = \begin{cases} 0 & z_1 < -L_{12} \\ \dfrac{k_1(z_1 + L_{12})}{L_{12} - L_{11}} & -L_{12} \le z_1 < -L_{11} \\ k_1 & -L_{11} \le z_1 < L_{11} \\ \dfrac{k_1(L_{12} - z_1)}{L_{12} - L_{11}} & L_{11} \le z_1 < L_{12} \\ 0 & L_{12} \le z_1 \end{cases} \tag{17}$$

For clarity, according to (15) and (17), the smooth saturation function $\sigma_{11}(z_1)$ and its derivative are drawn in Figs. 1*a* and *b*. As we can see, both $\sigma_{11}(z_1)$ and $(\mathrm{d}\sigma_{11}(z_1)/\mathrm{d}z_1)$ are continuous.

2. The definition of σ_{12} is

$$\sigma_{12}(z_2) = \begin{cases} 0 & z_2 < -L_{22} \\ \dfrac{(1-\varepsilon_0)(L_{22} + z_2)}{M_1}, & -L_{22} \le z_2 < -L_{21} \\ 1 & -L_{21} \le z_2 < L_{21} \\ \dfrac{(1-\varepsilon_0)(L_{22} - z_2)}{M_1} & L_{21} \le z_2 < L_{22} \\ 0 & L_{22} \le z_2 \end{cases} \tag{18}$$

where $L_{22} = M_2/k_2$, $L_{21} = L_{22} - M_1/(1-\varepsilon_0)$ $(0 < \varepsilon_0 < 1)$. Generally, ε_0 is chosen to be a very small positive number. Here, M_1, M_2 and k_2 are positive design parameters satisfying

$$M_2 > M_1 k_2/(1-\varepsilon_0) \tag{19}$$

which yields $L_{21} > 0$, so that $\sigma_{12}(z_2)$ is well defined. From (18), it is easy to check that the first-order derivative of

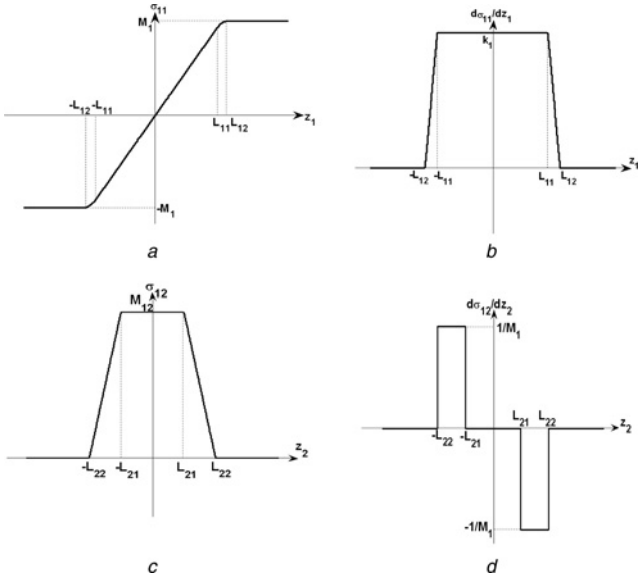

Fig. 1 *σ_{11}, σ_{12} and their first-order derivatives*

a σ_{11}
b $d\sigma_{11}/dz_1$
c σ_{12}
d $d\sigma_{12}/dz_2$

$\sigma_{12}(z_2)$ is as follows

$$\frac{d\sigma_{12}(z_2)}{dz_2} = \begin{cases} 0 & z_2 < -L_{22} \\ (1-\varepsilon_0)/M_1 & -L_{22} \le z_2 < -L_{21} \\ 0 & -L_{21} \le z_2 < L_{21} \\ -(1-\varepsilon_0)/M_1 & L_{21} \le z_2 < L_{22} \\ 0 & L_{22} \le z_2 \end{cases} \tag{20}$$

Graphically, σ_{12} and its first-order derivative are drawn in Figs. 1*c* and *d*. As we can see, the value of σ_{12} varies between zero and $1-\varepsilon_0$. Noting that $|\sigma_{11}| \le M_1$ and $\sigma_1 = \sigma_{11} \cdot \sigma_{12}$, one has

$$|\sigma_1| \le M_1 \tag{21}$$

which shows that σ_1 is bounded. In Assumption 3, we have stated the boundedness of $\dot{x}_{1d}$. Combining the boundedness of σ_1 and $\dot{x}_{1d}$ with (12), we know that α_1 is also bounded.

Remark 2: It should be noted that the virtual control law design in this paper is more flexible than that in [15]. In view of (14), the gain of virtual control $k_1\sigma_{12}(z_2)$ may vary between 0 and $1-\varepsilon_0$. Specifically, if σ_{12} is a constant, the virtual control law α_1 would be coherent to that in [15]. In other words, the controller proposed in this paper is more universal.

From (11)–(13), the derivative of z_1 can be derived as

$$\dot{z}_1 = z_2 + \alpha_1 - \dot{x}_{1d} = z_2 - \sigma_1 \tag{22}$$

Noting (22), from (9) and (12), one has

$$\begin{aligned} \dot{z}_2 &= \dot{x}_2 - \dot{\alpha}_1 \\ &= C \cdot \bar{u} - \theta_1 x_2 - \theta_2 S_f + \theta_3 + \Delta - \ddot{x}_{1d} \\ &\quad + \frac{\partial \sigma_{11}}{\partial z_1}\sigma_{12}\dot{z}_1 + \frac{\partial \sigma_{12}}{\partial z_2}\sigma_{11}\dot{z}_2 \\ &= -\theta_1 z_2 + \varphi(x)^{\mathrm{T}}\theta + C \cdot \bar{u} - \ddot{x}_{1d} \\ &\quad + \frac{\partial \sigma_{11}}{\partial z_1}\sigma_{12}(z_2 - \sigma_1) + \frac{\partial \sigma_{12}}{\partial z_2}\sigma_{11}\dot{z}_2 + \Delta \end{aligned} \tag{23}$$

where $\varphi = [-\alpha_1, -S_f, 1]^{\mathrm{T}}$, $\theta = [\theta_1, \theta_2, \theta_3]^{\mathrm{T}}$. Here, we need to design a bounded control law $\bar{u}$ such that it is within the prescribed interval $[-M_u, M_u]$. Let the control law be

$$\bar{u} = \bar{u}_a + \bar{u}_s \tag{24}$$

where $\bar{u}_a$ is the adaptive control term and $\bar{u}_s$ is the robust control term. The concept of ARC is to compensate the known part of the model dynamics by using $\bar{u}_a$ and to fight against various model uncertainties and disturbances by $\bar{u}_s$ [21]. In order to render $\bar{u}$ within the saturation limits, $\bar{u}_a$ and $\bar{u}_s$ should be bounded and designed as follows

$$\bar{u}_a = \frac{1}{C}\left(\ddot{x}_{1d} - \varphi^{\mathrm{T}}\hat{\theta} + \frac{\partial \sigma_{11}}{\partial z_1}\sigma_{12}\sigma_1\right) \tag{25}$$

in which the parameter estimate $\hat{\theta}$ is updated online whose adaptation law is given by

$$\dot{\hat{\theta}} = \mathrm{Proj}_{\hat{\theta}}(\Gamma\varphi z_2) \tag{26}$$

where Proj(•) represents the discontinuous projection operator. Its definition and properties can be seen in [22].

From the definition of φ, σ_{11}, σ_{12} and σ_1, we can conclude that $\bar{u}_a$ is bounded. More specifically, according to the Cauchy–Schwartz inequality, it follows that

$$\begin{aligned} |\bar{u}_a| \le \frac{1}{C}\Bigg(&\|\ddot{x}_{1d}\|_\infty + k_1 M_1 \cdot \\ &+ \sqrt{2(\dot{x}_{1d}^2 + M_1^2) + 2} \cdot \sqrt{\theta_{1\max}^2 + \theta_{2\max}^2 + \theta_{3\max}^2}\Bigg) \end{aligned} \tag{27}$$

The robust control term $\bar{u}_s$ is synthesised as

$$\bar{u}_s = -\sigma_2(z_2)/C \tag{28}$$

where σ_2 is a saturated function

$$\sigma_2(z_2) = \begin{cases} -M_2 & z_2 < -L_{22} \\ k_2 z_2 & -L_{22} \le z_2 < L_{22} \\ M_2 & L_{22} \le z_2 \end{cases} \tag{29}$$

where M_2 is designed as a positive constant. According to (29), $\bar{u}_s$ is bounded by

$$|\bar{u}_s| \le M_2/C \tag{30}$$

For clarity, the curve of $\sigma_2(z_2)$ is depicted in Fig. 2. From (24), (25) and (28), we have

$$\bar{u} = \frac{1}{C}\left(\ddot{x}_{1d} - \varphi^{\mathrm{T}}\hat{\theta} + \frac{\partial \sigma_{11}}{\partial z_1}\sigma_{12}\sigma_1 - \sigma_2(z_2)\right) \tag{31}$$

Noting (27) and (30), then

$$\begin{aligned} |\bar{u}| &\le \bar{u}_b(M_1, M_2, k_1, \theta_{\max}) \\ &= \frac{1}{C}\Bigg(\|\ddot{x}_{1d}\|_\infty + k_1 M_1 + M_2 \\ &\quad + \sqrt{2(\dot{x}_{1d}^2 + M_1^2) + 2} \cdot \sqrt{\theta_{1\max}^2 + \theta_{2\max}^2 + \theta_{3\max}^2}\Bigg) \end{aligned} \tag{32}$$

If the controller parameters M_1, M_2, k_1 and $\theta_{\max}$ are designed such that $\bar{u}_b(M_1, M_2, k_1, \theta_{\max}) \le M_u$, then the control input $u = \bar{u}$ will not cause saturation, which means that the

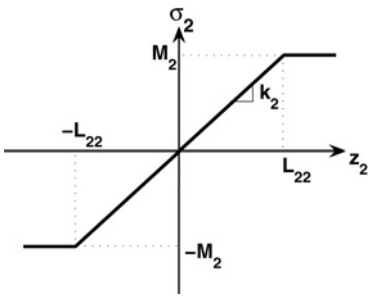

Fig. 2 *Curve of $\sigma_2(z_2)$*

doi: 10.1049/iet-cta.2010.0415

saturation non-linearity has no influence on the system as if it does not exist.

From (23) and (31), one has

$$\dot{z}_2 = -\theta_2 z_2 - (\varphi(x)^{\mathrm{T}}\tilde{\theta} + \Delta) + \frac{\partial \sigma_{11}}{\partial z_1}\sigma_{12} z_2 - \sigma_2(z_2) + \frac{\partial \sigma_{12}}{\partial z_2}\sigma_{11}\dot{z}_2 \tag{33}$$

Because of the boundedness of φ and Assumption 2, it can be assumed that

$$|\varphi^{\mathrm{T}}\tilde{\theta} + \Delta| \le h \tag{34}$$

where h can be regarded as the bound of the total effect of model mismatch and unmodelled uncertainties. With this assumption, we will prove later that $z_2(t)$ can be made uniformly bounded if the parameters are designed to satisfy certain conditions as follows

$$M_2 \ge h \tag{35a}$$

$$L_{21} > h/(k_2 - k_1) \tag{35b}$$

$$k_1 L_{11} > h/(k_2 - k_1) \tag{35c}$$

Now we have finished the design procedures of the proposed SARC. In summary, the proposed SARC consists of: (i) the control law given by (31), whose parameters satisfy (16), (19), (35a)–(35c) and $\bar{u}_b \le M_u$. (ii) the adaptation law given by (26).

From (32), we know that the purpose of introducing the saturated functions σ_{11} and σ_2 is to make the control law $\bar{u}$ within saturation limit. But here comes a problem: what is the functionality of σ_{12}? In view of (33), σ_{12} can attenuate the influence of $(\partial\sigma_{11}/\partial z_1)\sigma_{12}z_2$, since σ_{12} becomes zero when z_2 is larger than L_{22}. In the following section, we will demonstrate that the introduction of σ_{11}, σ_{12} and σ_2 into the SARC can make the close-loop system stable.

4 Stability proof and performance analysis

Define a set Ω_c as

$$\Omega_c = \left\{ z_1, z_2 : |z_1| \le \frac{h + \varepsilon_1}{k_1(k_2 - k_1)}, \quad |z_2| \le \frac{h + \varepsilon_2}{k_2 - k_1} \right\}$$

where $\varepsilon_1 < L_{11}k_1(k_2 - k_1) - h$, $\varepsilon_2 < L_{21}(k_2 - k_1) - h$, $\varepsilon_1 > \varepsilon_2 > 0$. Then we are going to prove that the error states can be steered into the set Ω_c by SARC in finite time.

Theorem 1: Suppose that the saturated adaptive robust controller proposed in Section 3 is applied to the plant (9). Then,

1. the controller guarantees that all signals in the close-loop system are bounded. Furthermore, the trajectory of the error states $[z_1, z_2]^{\mathrm{T}}$ reaches the prescribed set Ω_c in a finite time and stay within thereafter.
2. the steady state of the tracking error z_1 is bounded by $|z_1(\infty)| \le (h/k_1(k_2 - k_1))$.

Proof: The proof of (1) is divided into two parts: Part I, z_2 gets into the interval $[-(h + \varepsilon_2)/(k_2 - k_1), (h + \varepsilon_2)/(k_2 - k_1)]$ in a finite time. Part II, with this property of z_2, z_1 evolves into $[-(h + \varepsilon_1)/(k_1k_2 - k_1^2), (h + \varepsilon_1)/(k_1k_2 - k_1^2)]$ in a finite time.

Part I: The evolution of z_2 is discussed in three cases, that is, (i) $|z_2| > L_{22}$; (ii) $L_{21} < |z_2| \le L_{22}$; (iii) $(h + \varepsilon_2)/(k_2 - k_1) < |z_2| \le L_{21}$. To simplify this proof, the sets corresponding to the above three cases are defined as follows

$$\Omega_0 = \{z_1, z_2 : |z_2| > L_{22}\}$$
$$\Omega_1 = \{z_1, z_2 : L_{21} < |z_2| \le L_{22}\}$$
$$\Omega_2 = \{z_1, z_2 : (h + \varepsilon_2)/(k_2 - k_1) < |z_2| \le L_{21}\}$$
$$\Omega_3 = \{z_1, z_2 : |z_2| \le (h + \varepsilon_2)/(k_2 - k_1)\}$$

Case 1: When $|z_2| > L_{22}$, from (20), (22) and (32), we have $\sigma_{12} = 0$, $(\partial\sigma_{12}/\partial z_2) = 0$, $\sigma_2 = M_2$. Noting that $\theta_2 > 0$ (Assumption 1), according to (33) and (34), then

$$z_2\dot{z}_2 \le -\theta_2 z_2^2 + h|z_2| - M_2|z_2| \le -(M_2 - h)|z_2| \tag{36}$$

Since $M_2 \ge h$, (36) indicates that any trajectory with the initial state $[z_1(0), z_2(0)]^{\mathrm{T}}$ in Ω_0 will reach the set Ω_1 in a finite time t_{01}, which is bounded by

$$t_{01} \le \frac{z_2(0) - L_{22}}{M_2 - h} \tag{37}$$

Case 2: When $L_{21} < |z_2| \le L_{22}$, from (18), (20) and (29), it follows that $\sigma_{12} \le 1$, $|\partial\sigma_{12}/\partial z_2| = (1 - \varepsilon_0/M_1)$ and $\sigma_2 = k_2 z_2$. Noting that $\sigma_{11} \le M_1$, one has $|\partial\sigma_{12}/\partial z_2\sigma_{11}| \le 1 - \varepsilon_0$. In accordance to (26)

$$z_2\dot{z}_2 = -\theta_2 z_2^2 + (\varphi^{\mathrm{T}}\tilde{\theta} + \Delta)z_2 + \frac{\partial \sigma_{11}}{\partial z_1}\sigma_{12} z_2^2 - k_2 z_2^2 + \frac{\partial \sigma_{12}}{\partial z_2}\sigma_{11} z_2\dot{z}_2 \tag{38}$$

which yields

$$\left(1 - \frac{\partial \sigma_{12}}{\partial z_2}\sigma_{11}\right) z_2\dot{z}_2 = -\theta_2 z_2^2 + (\varphi^{\mathrm{T}}\tilde{\theta} + \Delta)z_2 + \frac{\partial \sigma_{11}}{\partial z_1}\sigma_{12} z_2^2 - k_2 z_2^2$$

Noting (34), since

$$\varepsilon_0 \le 1 - \frac{\partial \sigma_{12}}{\partial z_2}\sigma_{11} \le 2 - \varepsilon_0 \quad \text{and} \quad \frac{\partial \sigma_{11}}{\partial z_1}\sigma_{12} < k_1$$

we have

$$z_2\dot{z}_2 \le \frac{-\theta_2 z_2^2 + h|z_2| + k_1 z_2^2 - k_2 z_2^2}{(1 - (\partial\sigma_{12}/\partial z_2)\sigma_{11})} \le \frac{-(k_2 L_{21} - k_1 L_{21} - h)|z_2|}{2 - \varepsilon_0} \tag{39}$$

Owing to $k_2 L_{21} \ge k_1 L_{21} + h$, (39) indicates that any trajectory with the initial state $[z_1(0), z_2(0)]^{\mathrm{T}}$ in Ω_1 will reach the set Ω_2 in a finite time t_{12}. Moreover, the upper bound of the reaching time t_{12} is

$$t_{12} \le \frac{|z_2(0)|(2 - \varepsilon_0)}{k_2 L_{21} - k_1 L_{21} - h} \tag{40}$$

Case 3: When $(h+\varepsilon_2)/(k_2-k_1) < |z_2| \le L_{21}$, from (18), (20) and (29), we have $\sigma_{12}=1$, $(\partial\sigma_{12}/\partial z_2)=0$ and $\sigma_2 = k_2 z_2$. Noting $|z_2| > (h+\varepsilon_2)/(k_2-k_1)$, from (33) and (34), one has

$$\begin{aligned} z_2\dot{z}_2 &= -\theta_2 z_2^2 + (\varphi^{\mathrm{T}}\tilde{\theta}+\Delta)z_2 + \frac{\partial\sigma_{11}}{\partial z_1}z_2^2 - k_2 z_2^2 \\ &\le (\varphi^{\mathrm{T}}\tilde{\theta}+\Delta)z_2 - (k_2-k_1)z_2^2 \\ &\le -(h+\varepsilon_2-h)|z_2| \\ &= -\varepsilon_2|z_2| \end{aligned} \tag{41}$$

Owing to $\varepsilon_2 > 0$, (41) indicates that any trajectory with the initial state $[z_1(0),\ z_2(0)]^{\mathrm{T}}$ in Ω_2 reaches the set Ω_3 in a finite time t_{23}. Furthermore, the upper bound of the reaching time t_{23} is

$$t_{23} \le \frac{|z_2(0)|}{\varepsilon_2} \tag{42}$$

From the analysis of the above three cases, we know that the trajectory of the $[z_1,\ z_2]^{\mathrm{T}}$ steps into Ω_3 in a finite time, no matter where the initial states are. That means z_2 gets into the interval $[-(h+\varepsilon_2)/(k_2-k_1),(h+\varepsilon_2)/(k_2-k_1)]$ within a finite time.

Part II: After a finite time, $|z_2| \le (h+\varepsilon_2)/(k_2-k_1)$. Under this condition, we discuss the evolution of z_1 in two cases, that is, (i) $|z_1| > L_{11}$, and (ii) $(h+\varepsilon_1)/(k_1(k_2-k_1)) < |z_1| \le L_{11}$. For simplicity, the set Ω_4 is defined as

$$\Omega_4 = \{z_1, z_2 : |z_1| \le L_{11},\ |z_2| \le (h+\varepsilon_2)/(k_2-k_1)\}$$

Note that Ω_4 is a subset of Ω_3. From (22), one has

$$z_1\dot{z}_1 = z_1(z_2-\sigma_1) \tag{43}$$

Case 1: When $|z_1| > L_{11}$ and $|z_2| \le (h+\varepsilon_2)/(k_2-k_1)$, according to (14), (43) and $|z_2| \le (h+\varepsilon_2)/(k_2-k_1)$, the following inequality holds.

$$z_1\dot{z}_1 \le -\left(k_1 L_{11} - \frac{h+\varepsilon_2}{k_2-k_1}\right)|z_1| \tag{44}$$

Since $h+\varepsilon_2 < h+\varepsilon_1 < L_{11}k_1(k_2-k_1)$, (44) indicates that any trajectory with the initial states $[z_1(0),\ z_2(0)]^{\mathrm{T}}$ in Ω_3 will reach the set Ω_4 in a finite time t_{34}. Furthermore, the upper bound of the reaching time t_{34} is

$$t_{34} \le \frac{z_1(0)(k_2-k_1)}{L_{11}k_1(k_2-k_1)-h-\varepsilon_2} \tag{45}$$

Case 2: When $(h+\varepsilon_1/k_1(k_2-k_1)) < |z_1| \le L_{11}$ and $|z_2| \le (h+\varepsilon_2)/(k_2-k_1)$, according to (14) and (43)

$$\begin{aligned} z_1\dot{z}_1 &= -k_1 z_1^2 + z_1 z_2 \le -k_1 z_1^2 + \frac{h+\varepsilon_2}{k_2-k_1}|z_1| \\ &\le -\left(\frac{h+\varepsilon_1}{k_2-k_1} - \frac{h+\varepsilon_2}{k_2-k_1}\right)|z_1| = -\frac{\varepsilon_1-\varepsilon_2}{k_2-k_1}|z_1| \end{aligned} \tag{46}$$

Since $\varepsilon_1 > \varepsilon_2$, (46) indicates that any trajectory with the initial state $[z_1(0),\ z_2(0)]^{\mathrm{T}}$ in Ω_4 will reach Ω_c in a finite time t_{4c}, which is bounded by

$$t_{4c} \le \frac{z_1(0)(k_2-k_1)}{\varepsilon_1-\varepsilon_2} \tag{47}$$

Combining the analysis of the above two cases, any trajectory with the initial states in Ω_3 will reach Ω_c in finite time.

From the deduction in Part I and Part II, we arrive at the conclusion that no matter what the initial states are, the trajectory of $[z_1,\ z_2]^{\mathrm{T}}$ can be steered to Ω_c in a finite time. Therefore the states $[z_1,\ z_2]^{\mathrm{T}}$ are bounded. In addition, because of using the projection mapping, all the states of the adaptation law, that is, $\hat{\theta}_1$, $\hat{\theta}_2$ and $\hat{\theta}_3$ are bounded. Noting that α_1 is bounded and $x_2 = z_2 + \alpha_1$, we know that x_2 is also bounded. From the boundedness of z_1 and x_{1d}, x_1 is also bounded. Conclusively, all the states of the close-loop system are bounded. Hence, (1) of Theorem 1 has been proven. □

Now, we prove (2). According to the analysis of case (3) in Part I, after a finite time the tracking error z_2 satisfies

$$\begin{aligned} z_2\dot{z}_2 &= -\theta_2 z_2^2 + (\varphi^{\mathrm{T}}\tilde{\theta}+\Delta)z_2 + \frac{\partial\sigma_{11}}{\partial z_1}z_2^2 - k_2 z_2^2 \\ &\le (\varphi^{\mathrm{T}}\tilde{\theta}+\Delta)z_2 - (k_2-k_1)z_2^2 \\ &\le -\frac{k_2-k_1}{2}z_2^2 + h|z_2| - \frac{k_2-k_1}{2}z_2^2 \\ &\le -\frac{k_2-k_1}{2}z_2^2 + \frac{h^2}{2(k_2-k_1)} \end{aligned} \tag{48}$$

Define V_2 as $V_2 = (1/2)z_2^2$ and k_s as $k_s = k_2 - k_1$. From (48), the derivative of V_2 satisfies

$$\dot{V}_2 \le -k_s V_2 + \frac{h^2}{2k_s} \tag{49}$$

which yields

$$V_2(t) \le \exp(-k_s t)V_2(0) + \frac{h^2}{2k_s^2}[1-\exp(-k_s t)] \tag{50}$$

It indicates that the steady state of z_2 is bounded by $z_2(\infty) \le h/k_s$. Then, according to the first equation of (46), the steady state of the tracking error z_1 is bounded by $z_1(\infty) \le h/(k_1 k_s) = h/[k_1(k_2-k_1)]$.

Remark 3: From the proof of Theorem 1, we can see that if $|z_2(0)| > (h+\varepsilon_2)/(k_2-k_1)$, $|z_2|$ decreases monotonically, and the trajectory of $[z_1,\ z_2]^{\mathrm{T}}$ will reach the set $\Omega_3 = \{z_1,\ z_2 :\ |z_2| \le (h+\varepsilon_2)/(k_2-k_1)\}$ in finite time. Then the tracking error z_1 will decay to the neighbourhood of zero.

Theorem 2: With the saturated adaptive robust controller proposed in Section 3 applied to the plant (9), asymptotic output tracking can be achieved if the system is only subject to parametric uncertainty after a finite time, that is, $\Delta = 0$, $\forall \ge t_0$ for some t_0.

Proof: Define a positive definite function V_a as

$$V_a = (1/2)z_2^2 + (1/2)\tilde{\theta}^T\Gamma^{-1}\tilde{\theta}$$

According to Theorem 1, the trajectory of the states $[z_1,\ z_2]^{\mathrm{T}}$

doi: 10.1049/iet-cta.2010.0415

will enter Ω_c in finite time. If $\Delta = 0$, when $[z_1, z_2]^{\mathrm{T}} \in \Omega_c$, the derivative of V_a can be derived as

$$\begin{aligned}\dot{V}_a &= -\theta_2 z_2^2 + \varphi^{\mathrm{T}}\tilde{\theta} z_2 + \frac{\partial \sigma_{11}}{\partial z_1} z_2^2 - k_2 z_2^2 \\ &\quad + \tilde{\theta}^{\mathrm{T}} \Gamma^{-1} \mathrm{Proj}_{\hat{\theta}}(\Gamma \varphi z_2) \\ &\le -\theta_2 z_2^2 - (k_2 - k_1) z_2^2 \end{aligned} \tag{51}$$

which indicates that z_2 converges to zero asymptotically. Subsequently, the tracking error z_1 will also converge to zero asymptotically according to (22). The Theorem 2 is proved. □

5 Simulations

Consider the dynamic model given by (9) with the parameters selected as: $J = 0.1\ \mathrm{kg \cdot m^2}$, $B = 0.08\ \mathrm{N \cdot m^2/(rad/s)}$, $T_c = 0.07\ \mathrm{N \cdot m^2}$, $R_a = 5\ \Omega$, $K_T = 5\ \mathrm{N \cdot m^2/A}$, $K_E = 0.2\ \mathrm{V/(rad/s)}$, $T_l = 0.1\ \mathrm{N \cdot m^2}$, $M_u = 1\ \mathrm{V}$. The disturbance Δ is chosen as a uniformly distributed pseudo-random number with an amplitude less than 0.05 N/kg, that is, $\Delta = (0.1\ \mathrm{rand}(1) - 0.05)\ \mathrm{N/kg}$. Then the dynamic model of a servo system in the form of (9) can be derived as

$$\begin{cases} \dot{x}_1 = x_2 \\ \dot{x}_2 = 10 \cdot \bar{u} - 2.8x_2 - 0.7S_f + 1 + 0.1\,\mathrm{rand}\,(1) - 0.05 \\ y = x_1 \\ \bar{u} = \mathrm{sat}(u,\ 1) \end{cases} \tag{52}$$

The corresponding parameters of model (52) can be obtained as

$$\begin{aligned} C &= 10((\mathrm{rad/s^2})/\mathrm{v}), & \theta_1 &= 2.8(1/\mathrm{s}) \\ \theta_2 &= 0.7((\mathrm{rad/s^2})/(\mathrm{N \cdot m})), & \theta_3 &= 1(\mathrm{rad/s^2}) \end{aligned}$$

Assuming that these parameters are unknown, the parameter bounds are chosen as: $\theta_{\min} = [2.5,\ 0.5,\ 0.5]^{\mathrm{T}}$, $\theta_{\max} = [3,\ 1,\ 1.2]^{\mathrm{T}}$, $\delta = 0.1$. According to these prescribed bounds, by use of the design procedure in Section 3, the parameters of the SARC are synthesised as: $a = 500$, $k_2 = 200$, $M_2 = 2.3$, $\varepsilon_0 = 0.05$, $\Gamma = \mathrm{diag}([800,\ 160,\ 200])$. The continuous function S_f, which is used to approximate $\mathrm{sgn}(x_2)$, is selected as $S_f = (2/\pi)\mathrm{atan}(900x_2)$.

In the simulations, two cases are considered. Case 1: The tracking performance will be demonstrated with a point-to-point desired trajectory. Case 2: The stabilisation with large initial error is considered. The purpose of this configuration is to illustrate the anti-windup effect of the proposed SARC.

5.1 Case 1: point-to-point trajectory

The input signal is a point-to-point trajectory with a maximum angle of 0.2 rad, a maximum angular velocity of 0.4 rad/s, a maximum acceleration of 2 rad/s^2, as depicted in Fig. 3. The initial states of the plant (52) are set to zeros. With the aforementioned SARC parameters and the property of input signal, the upper bound of the control input $\bar{u}_{\mathrm{b}}$ can be computed according to (32) as

$$\begin{aligned} \bar{u} \le \bar{u}_{\mathrm{b}} &= \frac{1}{C}\left(\|\ddot{x}_{1d}\|_\infty + k_1 M_1 + M_2 \right. \\ &\quad \left. + \sqrt{2(\dot{x}_{1d}^2 + M_1^2) + 2} \cdot \sqrt{\theta_{1\max}^2 + \theta_{2\max}^2 + \theta_{3\max}^2} \right) \\ &= 0.1 \times \left(2 + 5 \times 0.1 + 2.3 \right. \\ &\quad \left. + \sqrt{2(0.4^2 + 0.1^2) + 2} \cdot \sqrt{3^2 + 1^2 + 1.2^2} \right) \\ &= 0.99739 < 1 \end{aligned} \tag{53}$$

According to (53), the control input is within the saturation limit, which means that controller wind-up is avoided. As shown in Fig. 4, the output tracking performance of SARC is desirable. We can see that the tracking error is less than 0.5×10^{-4} rad when simulation time is larger than 5 s, and the amplitude of tracking error decreases gradually as time increases. That is because the controller parameters are tuned on line by the adaptation law. The parameter estimates are shown in Fig. 5. As seen, the parameter

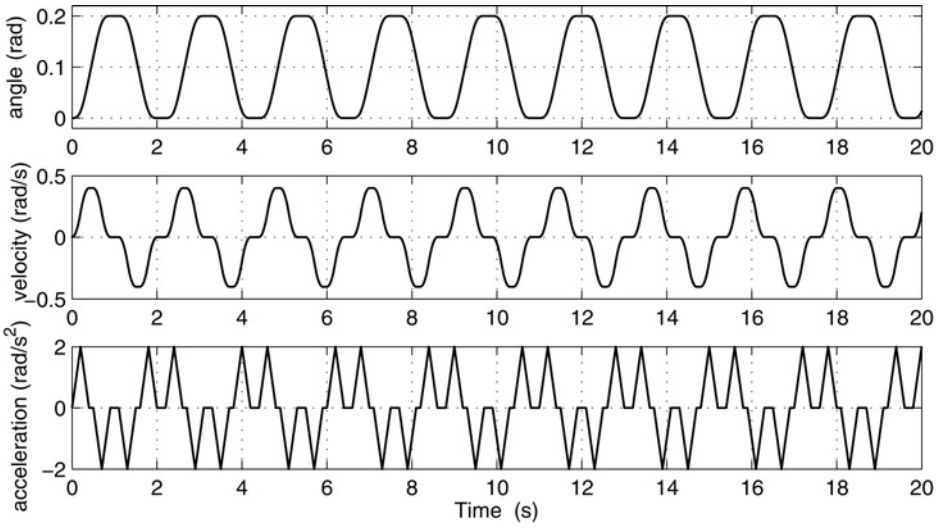

Fig. 3 *Point-to-point trajectory*

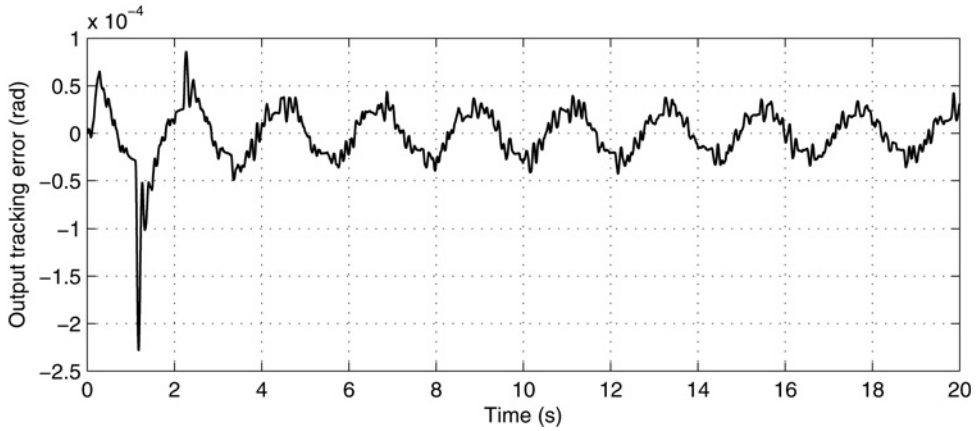

Fig. 4 *Output tracking error of SARC with a point-to-point trajectory as input*

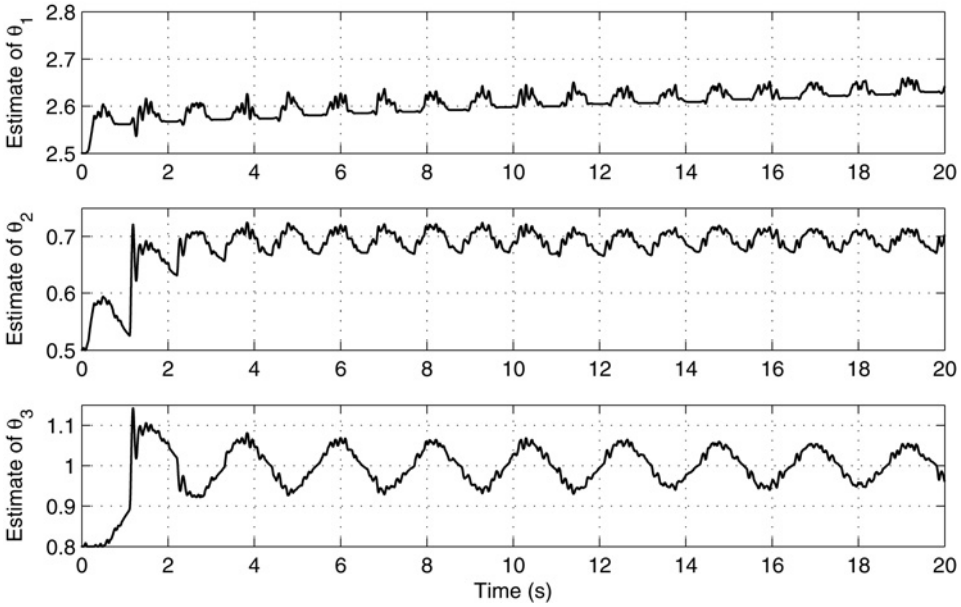

Fig. 5 *Parameter estimates in Case 1*

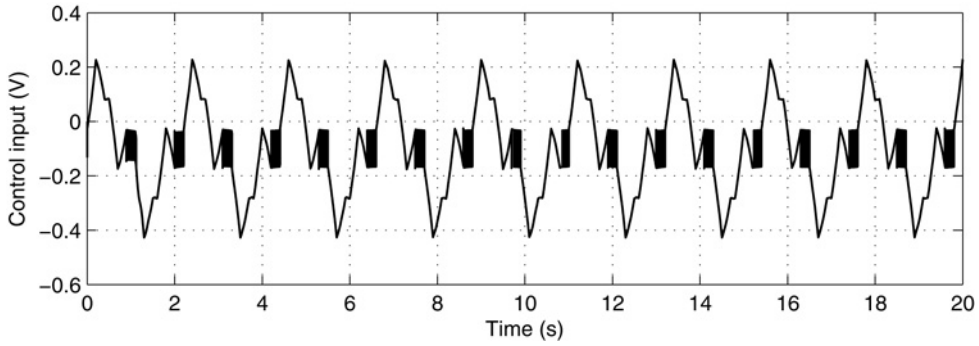

Fig. 6 *Control input of SARC in Case 1*

estimates evolve to the actual values gradually. Moreover, the estimates never exceed the prescribed bound owing to the use of projection operator. Fig. 6 shows the control input of SARC, whose amplitude is well within the preset bound $M_u = 1$, hence control input wind-up never occurs. This is the most distinguished feature of the proposed SARC.

5.2 Case 2: stabilisation with large initial error

In this case, the input signal is set to zero, while the initial condition of the plant is $[x_1, x_2] = [0.1, 0.2]$. The same controller parameters as those given in Subsection 5.1 are utilised in this case. It is obvious that the

doi: 10.1049/iet-cta.2010.0415

upper bound of the control input $\bar{u}_b$ can be computed according to (32) as

$$\bar{u} \le \bar{u}_b = \frac{1}{C}\left(\|\ddot{x}_{1d}\|_\infty + k_1 M_1 + M_2 + \sqrt{2(\dot{x}_{1d}^2 + M_1^2) + 2}\cdot\sqrt{\theta_{1\max}^2 + \theta_{2\max}^2 + \theta_{2\max}^2}\right)$$

$$= 0.1 \times \left(0 + 5 \times 0.1 + 2.3 + \sqrt{2(0^2 + 0.1^2) + 2}\cdot\sqrt{3^2 + 1^2 + 1.2^2}\right)$$

$$= 0.7607 < 1 \quad (54)$$

From (54), the control input satisfies $|\bar{u}| < M_u$, hence the control input wind-up is avoided.

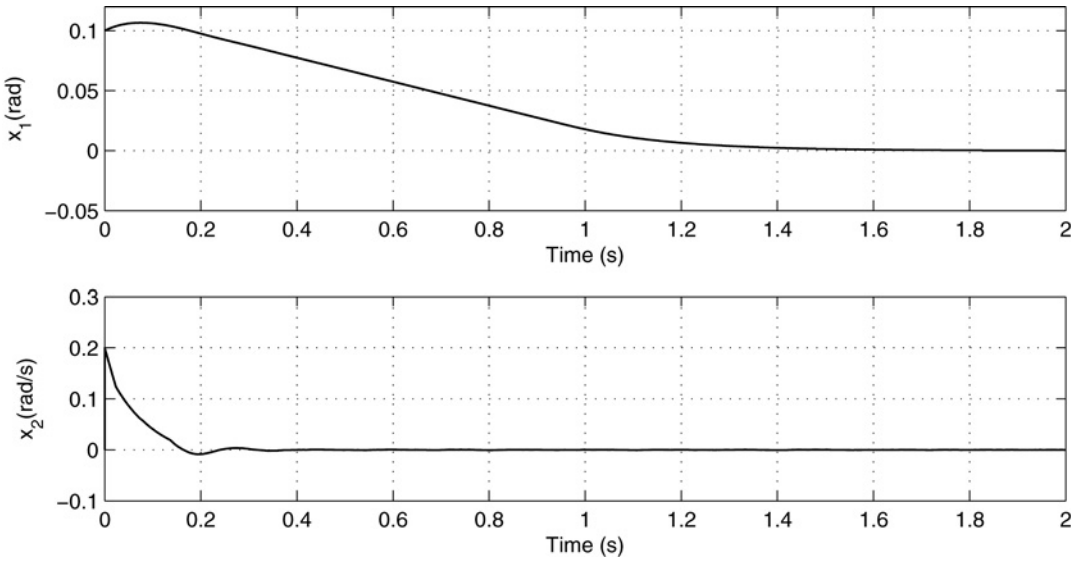

Fig. 7 *Trajectories of x_1 and x_2*

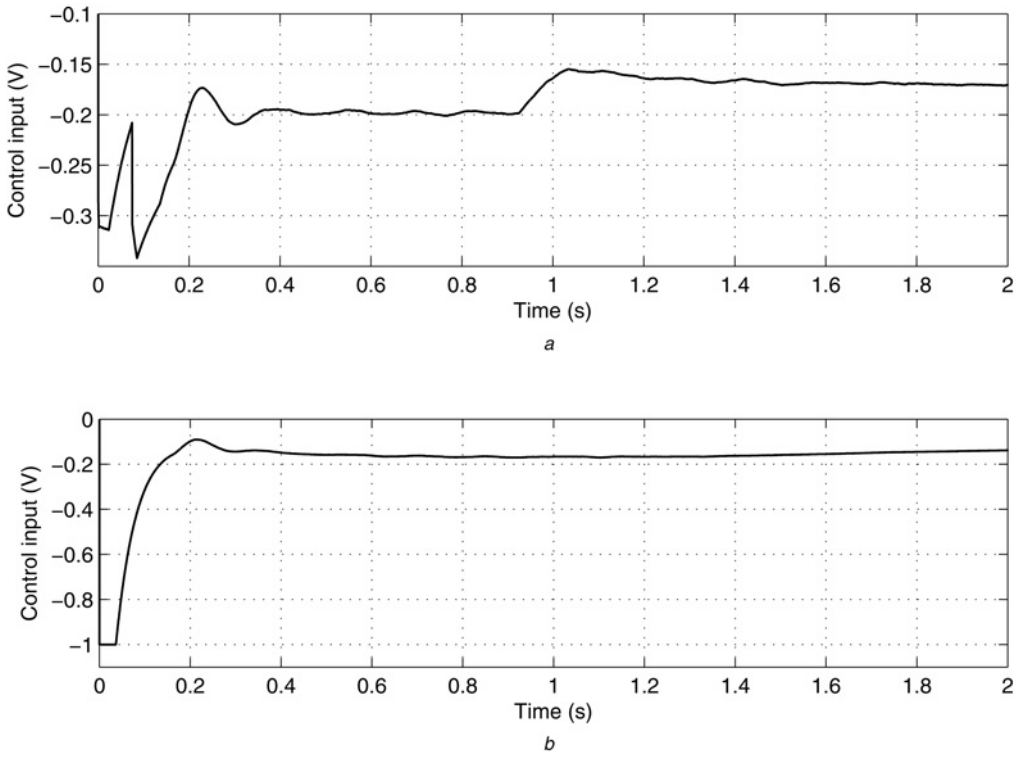

Fig. 8 *Control inputs of Case 2*

a SARC
b Ordinary ARC

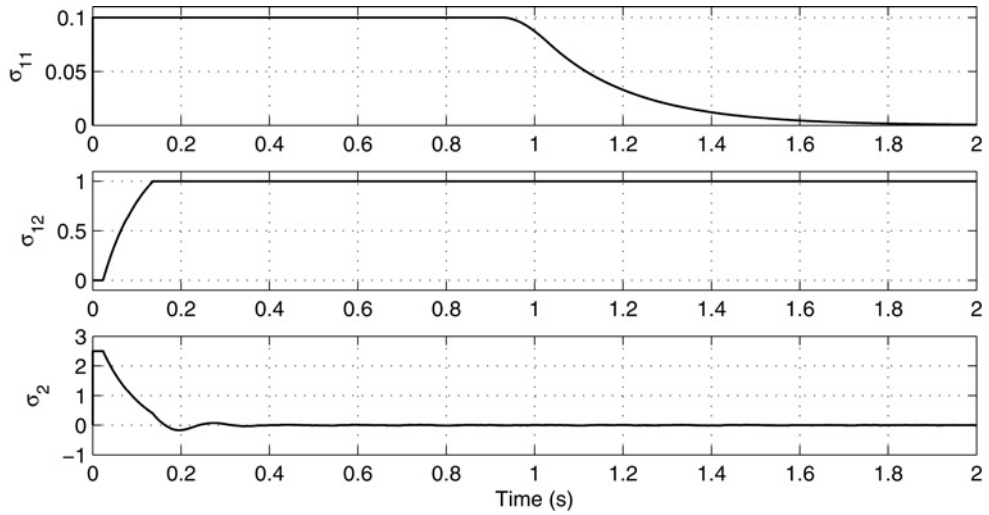

Fig. 9 *Trajectories of σ_{11}, σ_{12} and σ_2*

The state evolution of the close-loop system is depicted in Fig. 7. Both states are steered to zero by SARC. The control input of SARC is shown in Fig. 8*a*. As we can see, the control input is within the bound M_u, thus the saturation non-linearity has no influence on the close loop. This property is desired in our controller design.

It should be noted that if we let $\sigma_{11} = k_1 z_1$, $\sigma_{12} = 1$, $\sigma_2 = k_2 z_2$, then the SARC will turn to be the ordinary ARC. Fig. 8*b* shows the control input of the ordinary ARC with the same parameters as those of the aforementioned SARC. We find that the control input of the ordinary ARC is saturated at the outset of the control process. Although the large control input dose not certainly cause the close-loop system unstable, it is harmful to the machine health. Hence the control input amplitude of the SARC is favourable.

Fig. 9 shows the variations of σ_{11}, σ_{12} and σ_2. As is depicted, at the startup σ_{11} is saturated (i.e. $\sigma_{11} = M_1$) owing to the large magnitude of z_1. Besides, σ_{12} is small and σ_2 is saturated at the startup, since z_2 is larger than L_{21} in that phase. Noting $\sigma_1 = \sigma_{11}\sigma_{12}$, from (31), we know that the control input amplitude is restrained at the startup. As the states $[x_1, x_2]$ get close to the origin, the amplitudes of z_1 and z_2 decrease, therefore σ_{11} and σ_2 withdraw saturation, and σ_{12} equals to M_{12}. Then, the SARC turns to be an ordinary ARC and recover the performance of an ordinary ARC without saturation.

6 Conclusions

In this paper, we proposed a saturated adaptive robust controller for the DC servo system with input saturation. It embeds several saturation functions in the control law to keep the control input within the prescribed limit, and thus the control input wind-up is avoided. We proved that the proposed controller can not only assure the stability of the close-loop system, but also provide desirable control performance, that is, the tracking error can be steered to the neighbourhood of the origin. Moreover, asymptotic tracking can be achieved if the system is only subject to parametric uncertainty. In addition, the theoretical-analysis results were verified through simulation studies.

7 Acknowledgments

Contract/grant sponsor: Beijing Education Committee Cooperation Building Foundation Project; National Science Fund for Distinguished Young Scholars; contract/grant number: XK100070532; 60925011.

8 References

1 Zaccarian, L., Teel, A.R.: 'A common framework for anti-windup, bumpless transfer and reliable designs', *Automatica*, 2002, **38**, (10), pp. 1735–1744
2 Galeani, S., Teel, A.R.: 'On performance and robustness issues in the anti-windup problem'. Proc. IEEE Conf. on Decision and Control, Atlantis, 2004, pp. 5022–5027
3 Bernstein, D.S., Michel, A.N.: 'A chronological bibliography on saturating actuators', *Int. J. Robust Nonlinear Control*, 1995, **5**, (5), pp. 375–380
4 Grimm, G., Postlethwaite, I., Teel, A.R., *et al.*: 'Linear matrix inequalities for full and reduced order anti-windup synthesis'. Proc. American Control Conf., 2001, pp. 4134–4139
5 Hu, T., Lin, Z.: 'Composite quadratic lyapunov functions for constrained control systems', *IEEE Trans. Autom. Control*, 2003, **48**, (3), pp. 440–450
6 Teel, A.R.: 'Global stabilization and restricted tracking for multiple integrators with bounded controls', *Syst. Control Lett.*, 1992, **18**, (2), pp. 165–171
7 Xu, L., Yao, B.: 'Adaptive robust motion control of linear motors for precision manufacturing', *Mechatronics*, 2002, **12**, (4), pp. 595–616
8 Yao, B., Tomizuka, M.: 'Adaptive robust control of SISO nonlinear systems in a semi-strict feedback form', *Automatica*, 1997, **33**, (5), pp. 893–900
9 Yao, B.: 'High performance adaptive robust control of nonlinear systems: a general framework and new schemes'. Proc. IEEE Conf. on Decision and Control, 1997, pp. 2489–2494
10 Zhu, X., Tao, G., Yao, B., *et al.*: 'Adaptive robust posture control of parallel manipulator driven by pneumatic muscles with redundancy', *IEEE/ASME Trans. Mechatronics*, 2008, **13**, (4), pp. 441–450
11 Zhu, X., Tao, G., Yao, B., Cao, J.: 'Adaptive robust posture control of a parallel manipulator driven by pneumatic muscle', *Automatica*, 2008, **44**, (9), pp. 2248–2257
12 Zhong, J., Yao, B.: 'Adaptive robust precision motion control of a piezoelectric positioning stage', *IEEE Trans. Control Syst. Technol.*, 2008, **16**, (5), pp. 1039–1047
13 Yao, B., Majed, M.A., Tomizuka, M.: 'High performance robust motion control of machine tools: an adaptive robust control approach and comparative experiments', *IEEE Trans. Mechatronics*, 1997, **2**, (2), pp. 63–76
14 Gong, J.Q., Yao, B.: 'Global stabilization of a class of uncertain systems with saturated adaptive robust control'. Proc. IEEE Conf. on Decision and Control, Sydney, Australia, 2000, pp. 1882–1887

doi: 10.1049/iet-cta.2010.0415

15 Hong, Y., Yao, B.: 'A globally stable high-performance adaptive robust control algorithm with input saturation for precision motion control of linear motor drive systems', *IEEE/ASME Trans. Mechatronics*, 2007, **12**, (2), pp. 198–207
16 Hong, Y., Yao, B.: 'A globally stable saturated desired compensation adaptive robust control for linear motor systems with comparative experiments', *Automatica*, 2007, **43**, (10), pp. 1840–1848
17 Olsson, H., Astrom, K.J., Canudas de Wit, C., Gafvert, M., Lischinsky, P.: 'Friction models and friction compensation', *Eur. J. Control*, 1998, **4**, (3), pp. 176–195
18 Nasar, S.A., Boldea, I.: 'Linear electric motors: theory, design and practical applications' (Prentice Hall Press, Englewood Cliffs, NJ, 1987)
19 Tan, K.K., Huang, S.N., Dou, H.F., Lee, T.H., Chin, S.J., Lim, S.Y.: 'Adaptive robust motion control for precise trajectory tracking applications', *ISA Trans.*, 2001, **40**, (1), pp. 57–71
20 Lu, L., Chen, Z., Yao, B., *et al.*: 'Desired compensation adaptive robust control of a linear-motor-driven precision industrial gantry with improved cogging force compensation', *IEEE/ASME Trans. Mechatronics*, 2008, **13**, (6), pp. 617–624
21 Yao, B., Tomizuka, M.: 'Adaptive robust control of MIMO nonlinear systems in semi-strict feedback forms', *Automatica*, 2001, **37**, (9), pp. 1305–1321
22 Sastry, S., Bodson, M.: 'Adaptive control: stability convergence and robustness' (Prentice Hall Press, Englewood Cliffs, NJ, 1989)